Reactive Polytetrafluoroethylene/Polyamide Compounds. I. Characterization of the Compound Morphology with Respect to the Functionality of the Polytetrafluoroethylene Component by Microscopic and Differential Scanning Calorimetry Studies

G. Pompe, L. Häußler, P. Pötschke, D. Voigt, A. Janke, U. Geißler, B. Hupfer, G. Reinhardt, D. Lehmann

Institute of Polymer Research Dresden Leibniz, D-01005 Dresden, PF 12 04 11, Germany

Received 15 September 2004; accepted 3 February 2005
DOI 10.1002/app.22273
Published online in Wiley InterScience (www.interscience.wiley.com).

ABSTRACT: Compounds of electron-beam-irradiated polytetrafluoroethylene (PTFE) and polyamide (PA) were produced by reactive extrusion. During extrusion, both a breakdown process of the PTFE agglomerates and a chemical reaction between PTFE and PA took place. The morphology of the compounds was characterized with differential scanning calorimetry using fractionated crystallization, with atomic force microscopy and scanning electron microscopy, and with dynamic light scattering. The particle size of the dispersed PTFE phase decreased as the irradiation dose increased. A simple theoretical model of the breakdown process of PTFE agglomerates was made for the discussion of the development of the observed degree of dispersion.
 J Appl Polym Sci 98: 1308–1316, 2005

Key words: crystallization; morphology; polyamides; polytetrafluoroethylene (PTFE); reactive extrusion

INTRODUCTION

Compounds of polytetrafluoroethylene (PTFE) micropowder as a dispersed phase and polyamide (PA) as a matrix have been prepared by reactive extrusion[1] at processing temperatures of about 280°C, a temperature that is lower than the melting temperature of PTFE. The combination of the excellent sliding properties of PTFE with the advantage of effective processing is of interest for the production of injection-molded parts with complex geometry and good sliding properties.[2] During processing, the breakdown process of agglomerates of PTFE micropowder and transamidation as a chemical reaction between the reactive groups of the components take place. The processing conditions and, above all, the reactive groups of the PTFE component, produced by electron irradiation,[3] influence the degree of dispersion of the PTFE phase and the adhesion between PTFE and PA by the formation of PTFE/PA block copolymers.[4,5] Because the morphology of the dispersed phase and the compatibility between both components determine the final properties of the compound, these investigations are interesting for industrial applications of PTFE/PA compounds.[2,4]

Häußler et al.[6] studied PTFE/PA compounds with differential scanning calorimetry (DSC). The crystallization behavior of the PTFE phase shows the effect of fractionated crystallization. This effect has been observed and described in many publications.[7–10] The cause of this unusual crystallization behavior is the special size distribution of the dispersed, semicrystalline particles.[7,8] In addition to the bulklike crystallization at the temperature $T_{c,\mathrm{bulk}}$, a second crystallization step of the dispersed component can be observed at lower temperatures ($T_{c,i} < T_{c,\mathrm{bulk}}$) if the particle sizes (d_p) are smaller than a critical value ($d_{p,\mathrm{cr}}$). Häußler et al.[6] used the change observed in the fractionated crystallization behavior of the PTFE phase with respect to the irradiation dose for roughly assessing the morphology of the dispersed PTFE phase. From the observed tendency, it can be concluded that d_p of PTFE in the compound decreases as the irradiation dose is increased. This article presents both further DSC investigations into various compounds and microscopic studies using scanning electron microscopy (SEM) and atomic force microscopy (AFM). Additionally, dynamic light scattering (DLS) was applied. This method allowed a quantitative analysis of the particle size distribution of the dispersed PTFE phase in the compounds for the first time. The DLS results are discussed with respect to the other methods.

Correspondence to: L. Häußler (lili@ipfdd.de).

TABLE I
Characteristic Data of the Processing and Properties in the Initial State of the PTFE Micropowder Used for PTFE/PA Compounds with Commercial PTFE Types

Compound	T_{mass} (°C)/ screw configuration	$N_{e,r}$	X_n	Average d_p (μm)
C-MP1600/S12 (nonreactive)	275/S12	0.1×10^{-3}	3400	4–12
C-MP1100/S12	275/S12	1.2×10^{-3}	340	2–3

$N_{e,r}$ = sum of all functional —COF and —COOF end groups related to the number of the —CF_2— units; X_n = number of repeating —CF_2— units per molecule.

EXPERIMENTAL

Materials and processing

The matrix of the PTFE/PA compounds was polyamide PA6 Miramid SH3 (Leuna GmbH, Leuna, Germany) with a weight-average molecular weight of 18,000 g/mol. The reactive extrusion process was only practical with PTFE as a micropowder. Different types were used: commercial Zonyl MP 1600 as a regulated emulsion polymer with a very low concentration of carboxylic acid groups, commercial Zonyl MP 1100 as an irradiated emulsion polymer (DuPont, Wilmington, DE), and PTFE TF 2025 as an irradiated emulsion polymer (Dyneon GmbH, Burgkirchen, Germany). In the initial, nonirradiated state, the molecular weight of TF 2025 was estimated to be $\approx 10^6$ g/mol, and the average d_p value was $\approx$240 μm. Irradiation was performed at the ambient temperature in air with various doses. The irradiation caused chain scission in the molecules. Consequently, the molecular weight decreased. Simultaneously, carbonyl fluoride end groups (—COF) and, by hydrolysis during the posttreatment at 200°C for 1 h in air, carboxylic acid end groups (—COOH) were formed. Functionality $N_{e,r}$, as the sum of all reactive groups related to the CF_2— units, increased linearly as the dose was increased.[3] The PTFE micropowders consisted of agglomerates whose size distribution was dependent on the specific type. The particle size distribution of the PTFE micropowder in the initial state was determined by laser diffraction with a Helos particle size analyzer (Sympatec GmbH, Clausthal-Zellerfeld, Germany).

The compounds were processed in a ZSK 30 twin-screw extruder (Werner & Pfleiderer, Stuttgart, Germany). Two screw configurations (internal nomenclature S7 and S12) were applied; the shear rate of the S7 screw configuration was lower than that of S12. The throughput was 6 kg/h.

The mass temperature (T_{mass}), the screw configuration type (S7 or S12), and the PTFE type of the compounds are listed in Tables I and II for the compounds with a 50/50 (wt %/wt %) composition. In addition, some properties of the PTFE micropowder [polymerization degree (X_n) as a measure of the molecular weight,[3] $N_{e,r}$,[3] and characteristic values of d_p] determined in the initial state are given. The mass temperature of about 280°C is lower than the PTFE melting temperature. That means that most of the crystallites in the PTFE phase were not molten during the processing.

Methods of characterization

DSC

The DSC measurements were carried out on a DSC 7 (PerkinElmer, Ueberlingen, Germany) from −30 to 360°C in a nitrogen atmosphere with a scanning rate of ±20 K/min and a hold time of 0.5 min at a final temperature of 360°C. The run cycle was first heating/cooling/second heating. The calibration of the temperature and melting heat was performed with In and Pb standards. The samples were taken from the middle of the granules, and their mass was about 10 mg.

TABLE II
Characteristic Data of the Processing and Properties in the Initial State of the PTFE Micropowder Used for PTFE/PA Compounds with Irradiated PTFE TF 2025

Compound	T_{mass} (°C)/ screw configuration	Irradiation dose (kGy)	$N_{e,r}$	X_n[a]	Average d_p (μm)
C-500kGy/S7	285/S7	500	1.4×10^{-3}	572	Bimodal with a maximum at 2 and 13
C-1000kGy/S7	285/S7	1000	2.0×10^{-3}	290	Bimodal with a maximum at 2 and 13
C-1000kGy/S12	285/S12	1000	2.0×10^{-3}	290	Bimodal with a maximum at 2 and 13
C-2000kGy/S7	285/S7	2000	3.5×10^{-3}	176	Bimodal with a maximum at 2 and 13

$N_{e,r}$ = sum of all functional —COF and —COOH end groups related to the number of the —CF_2— units X_n = number of repeating —CF_2— units per molecule.
[a] Data from ref. 4.

Microscopic methods

For the microscopic studies, pieces of the granules were thermally treated in the DSC instrument up to 360°C and afterwards cooled to room temperature at the rate of −20 K/min. This procedure was chosen to compare SEM and AFM results with the results of the fractionated crystallization (DSC). The treated samples were embedded in an epoxy matrix.

SEM The cryofractured specimens were sputtered with gold and investigated with a Zeiss Leo VP 435 scanning electron microscope (LEO GmbH, Oberkochen, Germany).

AFM Ultramicrotomed cuts of the embedded pieces of the compounds were investigated with AFM. The measurements were performed in the tapping mode with a Dimension 3100 NanoScope IIIa (Veeco, Santa Barbara, CA) with Pointprobe silicon SPM sensors (Nanosensors, Neuchatel, Switzerland). The spring constant was about 3 N/m, and the resonance frequency was about 75 kHz. The tip radius was lower than 10 nm. The surface morphology (height image) and the adhesion behavior (phase image) were taken simultaneously. To get attraction contrast in the phase image, special scanning conditions (free amplitude < 20 nm, set-point amplitude ratio = 0.8) were used. Consequently, the bright areas in the phase images represent PTFE with low adhesion, and the dark areas represent PA with higher adhesion.

DLS

The PTFE particle size distribution was quantitatively analyzed by DLS with a Malvern PCS 4700 device (Malvern Instruments, Worcestershire, United Kingdom) equipped with a 25 mW He–Ne laser (model 127, Spectra Physics, Mountain View, CA). Highly diluted solutions of the granules of the PTFE/PA compounds, prepared with hexafluoroisopropanol (MERCK, Germany) as a solvent for PA, were investigated at 90°C. The particle size distribution was calculated with Malvern computing software in the monomodal mode.

RESULTS AND DISCUSSION

Theoretical approach of the breakdown mechanism

The particle size formed during melt processing is an important property of blends and compounds for their applications. There are already some models in the literature describing this process, such as that by Tokita.[11] Tokita explained the average size of melt droplets as a result of the equilibrium state between two competitive processes: the breakdown process and the coalescence. In the PTFE/PA compounds, the coalescence of mainly nonmolten PTFE can be ignored. In this way, the development of the morphology is only determined by the breakdown process of the nonmolten PTFE particles during the processing. This article describes a simple theoretical approach to the morphology development in the PTFE/PA compounds. The following two assumptions have been made for a simple approach:

1. The matrix viscosity (η_m) can be applied instead of the effective viscosity of the compound.[11] This is appropriate if the specific volume content, $v_d = V_d/V$ (volume of the dispersed phase/total volume), of the dispersed phase is small.
2. The particle shape can be assumed to be a sphere with the particle radius R_p. That means that the ratio of the particle surface (S_p) to the particle volume (V_p) is $S_p/V_p = 3/R_p$.

With these simplifications, the rate of the breakdown process (ν_{break}) can be estimated by an energy balance:

$$\nu_{\text{break}} = (dN/dt)/N \approx \eta_m(d\gamma/dt)^2/(e_{b,\text{bulk}} + 3\sigma_i/R_p \quad (1)$$

where N is the number of the particles, $d\gamma/dt$ is the shear rate, $e_{b,\text{bulk}}$ is the bulk fracture energy density, and σ_i is the interfacial tension between the PTFE particle and PA matrix.

The term $\eta_m(d\gamma/dt)^2$ describes the external work per particle volume and time transferred from the matrix to the particle. The denominator describes the fracture energy of the dispersed particle with respect to V_p and consists of $e_{b,\text{bulk}}$ of PTFE particles and the specific surface energy (σ_i). Relation (1) shows that ν_{break} decreases both with decreasing d_p and with increasing $e_{b,\text{bulk}}$. The attainable PTFE d_p value in the compounds can be estimated with relation (1) for the stationary stage with $\nu_{\text{break}} = 0$:

$$R_p \approx 3\sigma_i/[\eta_m(d\gamma/dt)^2 - e_{b,\text{bulk}}] \quad (2)$$

For a constant shear rate (unchanged processing conditions) and under the assumption of $\sigma_i \cong$ constant, d_p in the PTFE/PA compounds can be determined by the values of $e_{b,\text{bulk}}$. As a result of the special structure of the PTFE micropowder, there is a hierarchy of three varying values of $e_{b,\text{bulk}}$. The PTFE micropowders are agglomerates, which consist of so-called primary particles that are more or less loosely connected. The size of the primary particles is about 250 nm.[12] On the other hand, the primary particles are formed by crystallites with a size of about 22 nm.[13] The different kinds of particles are connected with various fracture strengths because of another internal structure, and so the value of $e_{b,\text{bulk}}$ increases from the agglomerates (R_p

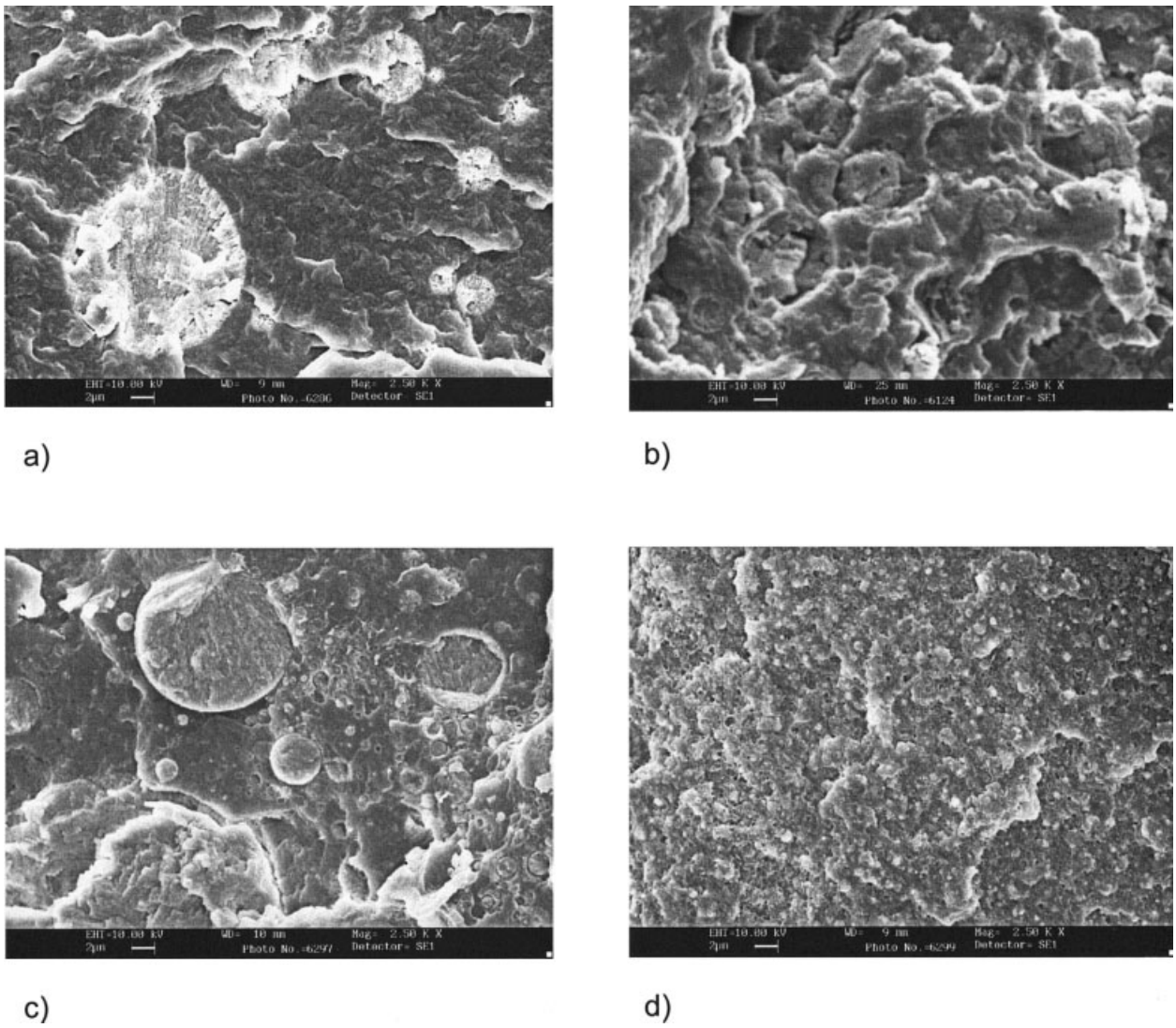

Figure 1 SEM images of cryofractures from thermally treated granules of (a) C-MP1600/S12, (b) C-MP1100/S12, (c) C-500kGy/S7, and (d) C-2000kGy/S7.

$> \approx$250 nm) via primary particles ($\approx$250 nm $> R_p >$ 22 nm) to crystallites ($R_p <$ 22 nm) because of $e_{b,\text{bulk}}$(agglomerate) $< e_{b,\text{bulk}}$(primary particle) $\ll e_{b,\text{bulk}}$(crystallite).

Additionally, the chain scissions, caused by irradiation and occurring above all in the amorphous parts, diminish $e_{b,\text{bulk}}$(agglomerate) and possibly also $e_{b,\text{bulk}}$(primary particle).

All these mechanisms determine the effectiveness of the breakdown process during the processing and accordingly the resulting size and morphology of the PTFE phase in the compounds.

Experimental results from microscopic methods

Cryofractures of thermally annealed granules of the compounds were investigated with SEM. Figure 1(a–d) shows SEM images for C-MP1600/S12, C-MP1100/S12, C-500kGy/S7, and C-2000kGy/S7. The images of the compounds with the commercial micropowders do not permit a more detailed interpretation. However, it can be seen that the fracture path partially goes through the PTFE particles in the case of C-MP1600/S12 [Fig. 1(a)]; this is discussed in more detail in the second part of this series.[6] The compounds produced with the same PTFE type irradiated with various doses [Fig. 1(c,d)] show clearly that d_p decreases as the irradiation dose increases. d_p in C-500kGy/S7 varies over a broad range from less than 1 μm up to 7 μm, whereas a very homogeneous particle size distribution with an average value lower than 1 μm can be observed in the C-2000kGy/S7 compound.

The proof that the dispersed phase in the compounds consists of PTFE was given by Grupper et

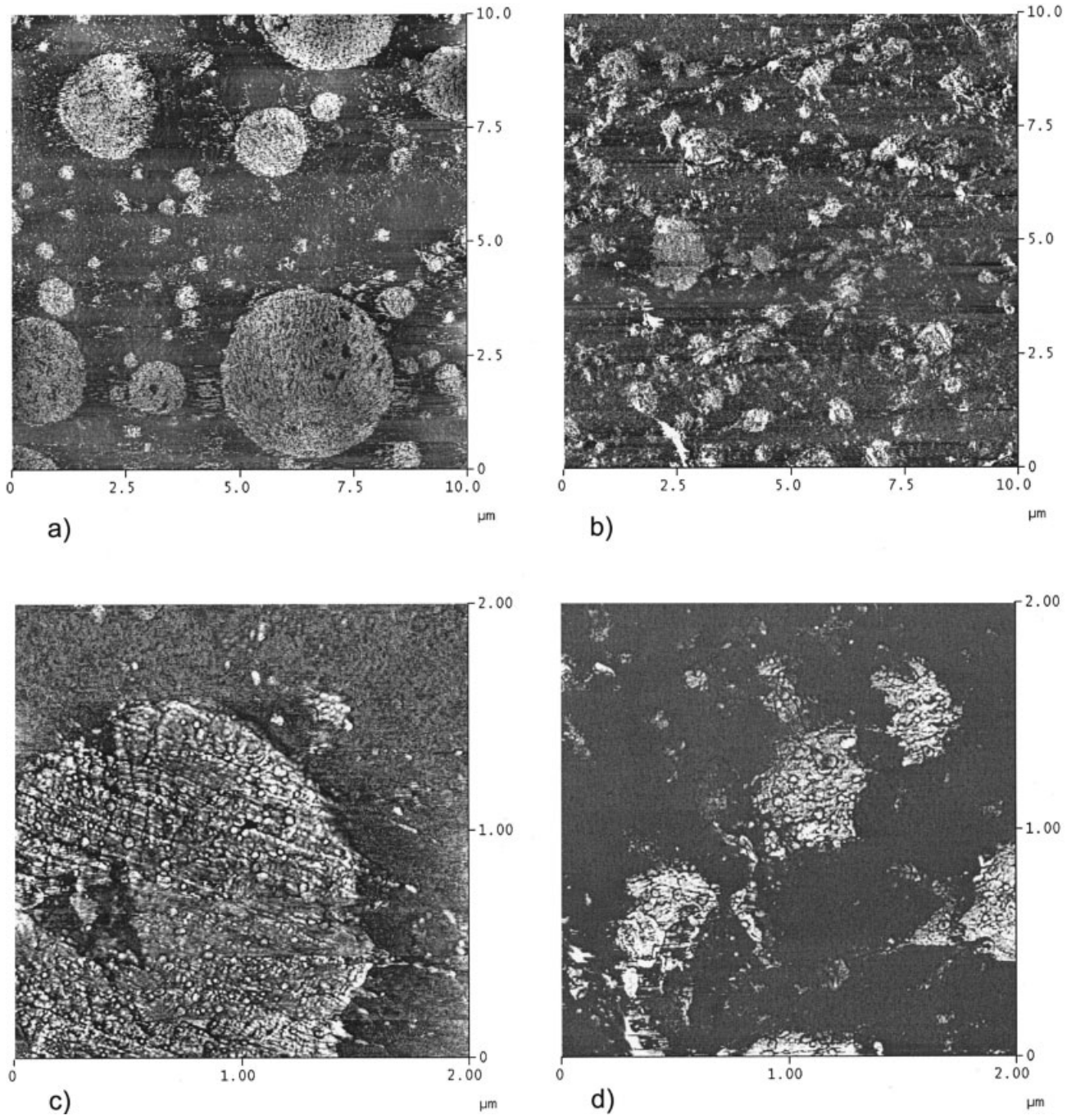

Figure 2 AFM phase images of microtome-cut surface of granules thermally treated in DSC: (a,c) C-1000kGy/S12 and (b,d) C-2000kGy/S7 (the magnification in parts c and d is 5 times higher than that in parts a and b).

al.,[14] who used transmission electron microscopy combined with electron energy loss spectroscopy.

In Figure 2(a–d), AFM phase images of cut surfaces of thermally treated granules of the C-1000kGy/S12 and C-2000kGy/S7 compounds are shown at various degrees of magnification. In the C-1000kGy/S12 compound [Fig. 2(a)], a remarkable number of particles with $d_p < 1$ μm can be observed among particles of about 4 μm, whereas in the C-2000kGy/S7 compound [Fig. 2(b)], all particles are smaller than 1 μm. The result of C-2000kGy/S7 is in agreement with that observed for cryofractures [Fig. 1(d)]. A direct comparison with the PTFE d_p values in C-1000kGy/S12 is not possible. However, the results correspond to expectations. It can also be observed that the spherical shape of the PTFE particles found in compounds with lowly irradiated PTFE [Fig. 2(c)] disappears in compounds with highly irradiated PTFE. The PTFE particles of the C-2000kGy/S7 compound [Fig. 2(d)] look like fractured parts of the agglomerates.

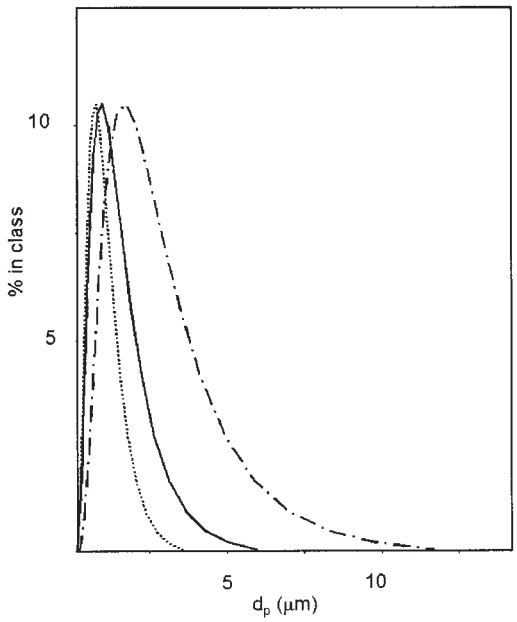

Figure 3 Particle size distribution of (- · -) C-MP1100/S12, (—) C-500kGy/S7, and (· · ·) C-2000kGy/S7, as determined by DLS.

The particle size distribution of the pure, irradiated PTFE micropowders is almost the same for irradiation doses from 500 to 2000 kGy (see Table II). Therefore, the varying particle size distribution observed in the compounds results from the breakdown process of the PTFE agglomerates during the extrusion. The development of the morphology of the C-500kGy/S7 and C-2000kGy/S7 compounds, produced with the same screw configuration (so-called S7), shows that the effectiveness of the breakdown process improves as the irradiation dose is increased. This can be explained by eq. (2), including the decrease of $e_{b,\text{bulk}}$ of the PTFE agglomerates, as a direct result of the chain scissions of PTFE molecules in the amorphous phase by the irradiation.

Particle size distribution (DLS)

Figure 3 shows the particle size distribution of the C-MP1100/S12, C-500kGy/S7, and C-2000kGy/S7 compounds after the same sedimentation time of about 60 min. Both the width and asymmetry of the particle size distribution as well as the average d_p value decrease from C-MP1100/S12 via C-500kGy/S7 to C-2000kGy/S7. The DLS results are in very good agreement with the behavior observed by SEM and AFM; an almost symmetrical particle size distribution and the average d_p value of about 820 nm obtained for C-2000kGy/S7 are very interesting.

Results of the fractionated crystallization

The heat flows of the cooling and second heating scans of compound C-500kGy/S7 are shown in Figure 4(a). The melting and crystallization of the PA component show the normally expected behavior. The PA crystallinity in the compounds is not changed into the limit of error with respect to the PTFE type or the composition of the compounds.

The crystallization behavior of the PTFE phase, shown in Figure 4(b), is remarkable. In addition to the bulklike crystallization step, a second one occurs at a lower temperature. That is the phenomenon of fractionated crystallization.[6–10] The extrapolated onset temperature ($T_{c,o}$) and the maximum temperature ($T_{c,m}$) of the bulk and fractionated exothermic crystallization peak are marked in Figure 4(b). The degree of fractionated crystallization [$h_{c,\text{frac}}$ (%)] of the dispersed PTFE phase is calculated as follows:

$$h_{c,\text{frac}} = 100[\Delta H_{c,\text{frac}}/(\Delta H_{c,\text{bulk}} + \Delta H_{c,\text{frac}})] \quad (3)$$

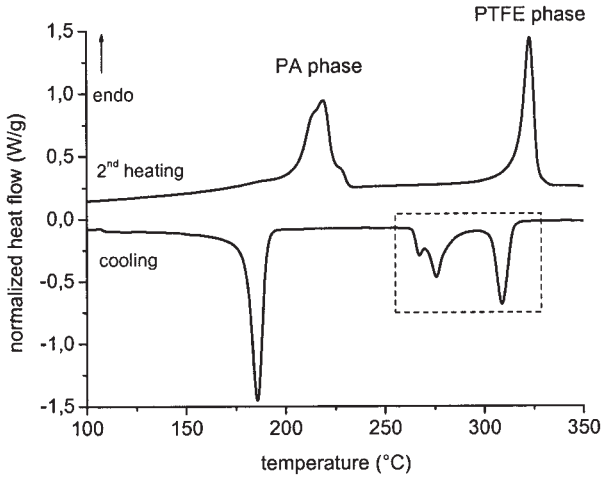

(a)

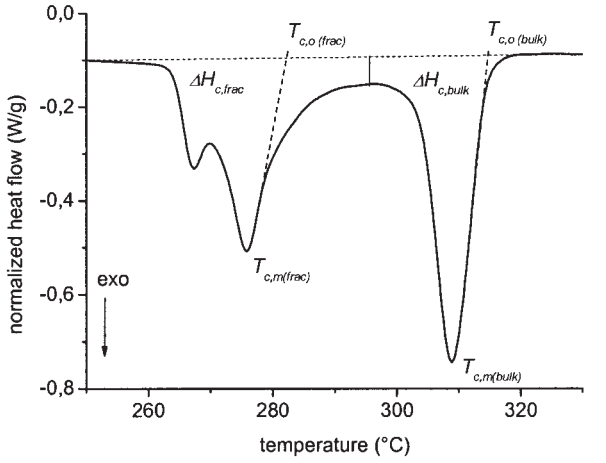

(b)

Figure 4 (a) Overview of the DSC cooling and second heating runs of the C-500kGy/S7 granule (rate = 20 K/min) and (b) crystallization of the PTFE phase of the C-500kGy/S7 granule in detail.

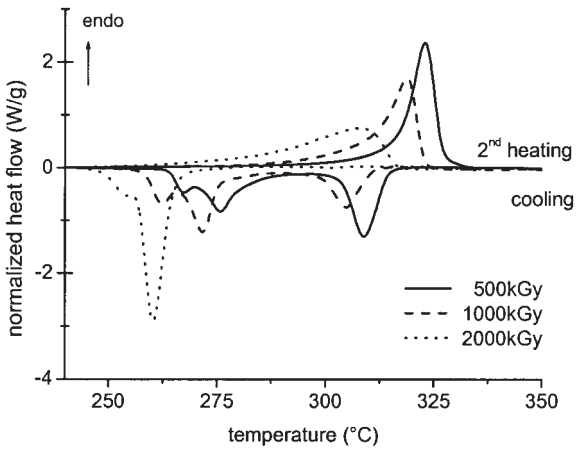

Figure 5 Cooling and second heating runs for the characterization of the influence of the irradiation dose on the crystallization and melting behavior of the PTFE phase in the C-500kGy/S7, C-1000kGy/S7, and C-2000kGy/S7 compounds.

where $\Delta H_{c,\text{bulk}}$ is the transition heat of the bulk crystallization step and $\Delta H_{c,\text{frac}}$ is the transition heat of the fractionated crystallization step.[9]

Figure 5 shows the heat flows of the crystallization and the following melting of the dispersed PTFE component in the compounds at various irradiation doses. Three characteristic features can be observed:

1. The qualitative behavior of the compounds with respect to the irradiation dose is similar to that in the pure, irradiated state of PTFE concerning the shift of melting and crystallization peak temperatures to lower values (decrease in the molecular weight), as shown by Häußler et al.[6]
2. The shape of the fractionated crystallization peak of the PTFE/PA compounds indicates a two-step crystallization. The contributions of both steps vary with respect to the irradiation dose. This is a special effect only observed with PA6 Miramid SH3 as the matrix. This interesting behavior can be explained in correlation to the degree of dispersion, as discussed in the appendix.
3. $h_{c,\text{frac}}$ increases as the irradiation dose of PTFE increases. This behavior reflects quite well the development of d_p of PTFE observed by the microscopic methods and DLS. Table III lists the values of $h_{c,\text{frac}}$ and the characteristic values of the particle size distribution determined by DLS. The highest value of $h_{c,\text{frac}}$ (98%) was found for C-2000kGy/S7, the compound with the most homogeneous particle size distribution and the smallest average d_p value (ca. 820 nm). This result confirms that fractionated crystallization can be used to assess the size distribution of the dispersed PTFE phase in the PTFE/PA compounds.[6] The simple preparation of samples for the DSC method is an important advantage in comparison with the microscopic methods. However, microscopic and/or DLS investigations are necessary for quantitative values of d_p. The quantitative value of the particle size distribution of the compounds and the value of $h_{c,\text{frac}}$ allow a rough estimate of $d_{p,\text{cr}}$.[9] PTFE particles smaller than $d_{p,\text{cr}}$ cannot crystallize at the temperature observed in the bulk state. For the C-2000kGy/S7 compound, the average PTFE d_p value amounts to 820 nm, and $h_{c,\text{frac}}$ is ≈98%. That means there are almost no PTFE particles that can crystallize at the bulk crystallization temperature. As can be seen in Figure 3, d_p of PTFE up to 7 μm can be observed in the C-500kGy/S7 compound. $h_{c,\text{frac}}$ is ≈50%. These results for both compounds permit a rough estimate of $d_{p,\text{cr}}$ to ≤1 μm.

Finally, the characteristic crystallization temperatures $T_{c,o}$ and $T_{c,m}$ of the PTFE crystallization processes in the compounds should be discussed. The values are listed in Table IV, and the dependence of $T_{c,m}$ on the PTFE type and the irradiation dose is shown in Figure 6. The values determined for pure PTFE micropowders in the initial state are also plotted for comparison. The values of the PTFE part with bulk behavior in the

TABLE III
Comparison of DLS Results and $h_{c,\text{frac}}$

Compound	Average d_p (μm)	Minimum and maximum values at class 5% (μm)	Asymmetry of particle distribution at class 5%	$h_{c,frac}$ (%)
C-MP1600/S12	Not determinable	Estimated 2–13	Not determinable	0.5
C-MP1100/S12	1.9	0.7–4.2	1.9	17
C-500kGy/S7	1.0	0.3–3	2.8	48
C-1000kGy/S7	Not determined	—	—	74
C-1000kGy/S12	Not determined	—	—	95
C-2000kGy/S7	0.82	0.3–1.3	1	98

compounds are nearly equal to those observed in pure PTFE. Both bulklike crystallization and what is called fractionated crystallization show the same slope with respect to $T_{c,m}$ versus the PTFE type and the irradiation dose, respectively. From that, it can be concluded that only the changed nucleation is responsible for the phenomenon of the fractionated crystallization process.

CONCLUSIONS

The degree of the dispersion of the PTFE phase in reactive PTFE/PA compounds has been investigated with respect to the irradiation doses and functionality of the PTFE component. DLS and fractionated crystallization determined by DSC were applied in addition to microscopic methods (SEM and AFM). The results of the fractionated crystallization of the dispersed PTFE phase were suitable for assessing the degree of dispersion.

The results of all the methods used show that the irradiation dose of PTFE is responsible for the effectiveness of the breakdown process during reactive extrusion. In this respect, the irradiation dose mainly determines the degree of the dispersion of the PTFE phase in the compound. The d_p values of the pure, irradiated PTFE, which vary from 2 to 10 μm, decrease strongly during the processing of the PTFE/PA compound. In the C-2000kGy/S7 compound with PTFE irradiated with 2000 kGy, the particle size distribution is very homogeneous, and the average value amounts to 820 nm. A simple model of the breakdown process given in this article can qualitatively explain the influence of the irradiation dose on the degree of the dispersion.

The expected influence of the shear rate on the degree of the dispersion could be confirmed by the results of the C-1000kGy/S7 and C-1000kGy/S12 compounds produced by various shear rates with the same PTFE type. The higher shear rate of what is called the S12 screw configuration results in $h_{c,\mathrm{frac}}$ = 95%, which is higher than the value of 74% when the S7 screw configuration is used.

TABLE IV
Characteristic Crystallization Temperatures of the PTFE Component in the Granules

Compound	$T_{c,o}$ (bulk) (°C)	$T_{c,m}$ (bulk) (°C)	$T_{c,o}$ (fract, first step) (°C)	$T_{c,m}$ (fract) (°C)
C-MP1600/S12	315	312	273	271
C-MP1100/S12	313	310	270	263
C-500kGy/S7	313	309	282	267
C-1000kGy/S7	312	308	273	267
C-1000kGy/S12	312	308	275	268
C-2000kGy/S7	306	302	265.5	257

Cooling rate = 20 K/min.

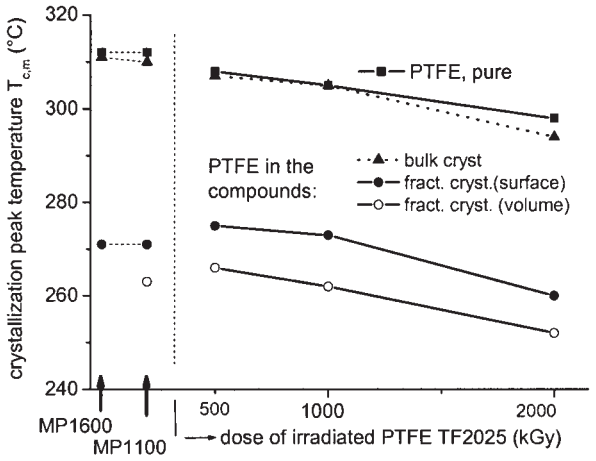

Figure 6 $T_{c,m}$ of PTFE in the initial state of the PTFE micropowder and in the compound granules versus the PTFE type and irradiation dose (cooling rate = 20 K/min).

The authors are grateful to U. Lappan for the data on the polymerization degree and functionality of the PTFE types used in the PTFE/PA compounds and to D. Jehnichen for the values of the crystallite size determined by WAXS. The authors thank U. Lappan and D. Fischer for their helpful discussions.

APPENDIX: EXPLANATION OF THE TWO-STEP FRACTIONATED CRYSTALLIZATION OF THE DISPERSED PTFE PHASE IN PTFE/PA6 MIRAMID SH3 COMPOUNDS

The behavior of the fractionated crystallization step of the PTFE/PA compounds with PA6 Miramid SH3 as the matrix, shown in Figure 5, indicates a two-step process. Normally, the fractionated crystallization peak is a one-step process.[8–10] When other PA types are used as the matrix, such as PA6 Ultramid B3, PA6 Ultramid B5 (BASF, Ludwigshafen, Germany), and PA12,[6] instead of PA6 Miramid SH3, the fractionated crystallization peak of the PTFE/PA compounds is a one-step process only.

Better insight into the behavior of the two-step crystallization effect with respect to the irradiation dose can be achieved if the change in the crystallization temperature caused by irradiation is eliminated by the shifting of the heat flows (see Fig. 5) by corresponding values on the temperature axis. The result of this manipulation is shown in Figure A.1. The first part of the fractionated crystallization step starting at higher temperatures becomes stronger, and the second process starting at lower temperatures is reduced as the dose increases. These tendencies correlate to $h_{c,\mathrm{frac}}$. The following hypothesis can be formulated: The first part of the fractionated crystallization step in the

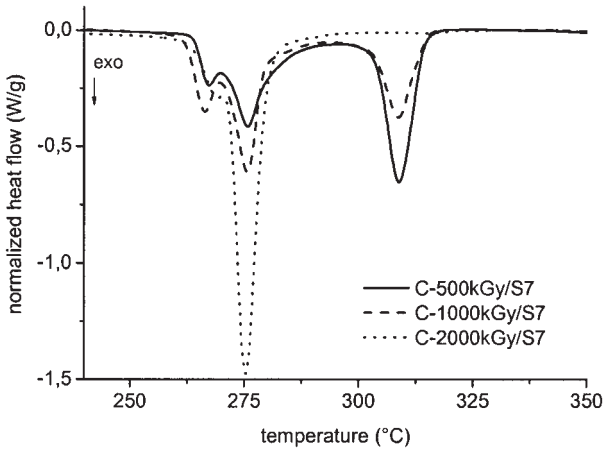

Figure A.1 Cooling runs for the characterization of the influence of the irradiation dose on the crystallization behavior of the PTFE phase in the C-500kGy/S7, C-1000kGy/S7, and C-2000kGy/S7 compounds (in comparison with Fig. 5, the temperatures were shifted for a suitable representation).

finely dispersed PTFE particles starts from the surface, caused by the nucleating effect of the surrounding molten PA6 Miramid SH3 matrix. Afterwards, the crystallization takes place inside the PTFE particles, starting from heterogeneous nuclei in the PTFE phase. As the irradiation dose is increased, $h_{c,\mathrm{frac}}$ increases, and the average d_p value decreases. The decreasing d_p value results in a different reduction in V_p ($\propto R_p^3$) and S_p ($\propto R_p^2$). Consequently, the first step starting from the particle surface becomes stronger in comparison with the second crystallization step, which starts inside the particle.[1] This is in agreement with the observed behavior.

References

1. Ger. Pat. DE 198 23 609 (1998).
2. Hupfer, B.; Lehmann, D.; Reinhardt. G.; Lappan, U.; Geißler, U.; Lunkwitz, K.; Kunze, K. Kunststoffe 2001, 91, 96.
3. Häußler, L.; Pompe, G.; Lehmann, D.; Lappan, U. Macromol Symp 2001, 164, 411.
4. Lappan, U.; Fuchs, B.; Geißler, U.; Scheler, U.; Lunkwitz, K. Polymer 2002, 43, 4325.
5. Lehmann, D.; Hupfer, B.; Lappan, U.; Pompe, G.; Häußler, L.; Jehnichen, D.; Janke, A.; Geissler, U.; Reinhardt, G.; Lunkwitz, K.; Franke, R.; Kunze, K. Des Monomers Polym 2002, 5, 317.
6. Pompe, G.; Häußler, L.; Adam, G.; Eichhorn, K.-J.; Janke, A.; Hupfer, B.; Lehmann, D. J Appl Polym Sci 2005, 98, 1317.
7. Frensch, H.; Harnischfeger, P.; Jungnickel, B.-J. In Multiphase Polymers: Blends and Ionomers; Utracki, L. A.; Weiss, R. A., Eds.; ACS Symposium Series 395; American Chemical Society: Washington, DC, 1989; Chapter 5.
8. Frensch, H.; Jungnickel, B.-J. Colloid Polym Sci 1989, 267, 16.
9. Everaert, V.; Groeninckx, G.; Aerts, L. Polymer 2000, 41, 1409.
10. Pompe, G.; Pötschke, P.; Pionteck, J. J Appl Polym Sci 2002, 86, 3445.
11. Tokita, N. Rubber Chem Technol 1977, 50, 292.
12. Lehmann, D.; Hupfer, B.; Lappan, U.; Geissler, U.; Reinhardt, G.; Pompe, G.; Häußler, L.; Janke, A.; Jehnichen, D.; Lunkwitz, K.; Franke, R.; Kunze, K. In Lubricants, Materials, and Lubrication Engineering, Proceedings of the 13th International Colloquium on Tribology; Bartz, W. J.; Ed.; Technische Akademie Esslingen: Ostfildern, Germany, 2002; Vol. 3, p 2309.
13. Ebnesajjad, S. Non-Melt Processible Fluoroplastics; Plastics Design Library: Norwich, CT, 2000; Vol. 1, p 135.
14. Grupper, A.; Wilhelm, P.; Kothleitner, G.; Eichhorn, K.-J.; Pompe, G. Macromol Symp 2004, 205, 171.